Structural Analysis and CO_2 Chemisorption Study on Nonstoichiometric Lithium Cuprates ($Li_{2+x}CuO_{2+x/2}$)

Luis M. Palacios-Romero,[†] Enrique Lima,[†,‡] and Heriberto Pfeiffer*,[†]

Instituto de Investigaciones en Materiales, Universidad Nacional Autónoma de México, Circuito exterior s/n CU, Del. Coyoacán, CP 04510, México DF, Mexico, and Departamento de Química, Universidad Autónoma Metropolitana, Iztapalapa, Av. San Rafael Atlixco 186, Col. Vicentina, Apdo. Postal 55-532, CP 09340, México DF, Mexico

Received: September 25, 2008; Revised Manuscript Received: November 6, 2008

Lithium cuprate (Li_2CuO_2) was prepared by solid state reaction, using different quantities of lithium excess, which produced nonstoichiometric ceramics, $Li_{2+x}CuO_{2+x/2}$. These ceramics were characterized by X-ray diffraction, transmission and scanning electron microscopies, solid state nuclear magnetic resonance, and atomic absorption. The results obtained showed that lithium excess is located mainly into the Li_2CuO_2 interlayers forming nanoparticles of a different phase, perhaps lithium oxide. Additionally, the lithium excess produced morphological changed at a micrometric and nanometric levels. As lithium excess increased, the particle size increased as well and it formed some kind of filament-like structures. It was explained in terms sintering, due to the high mobility of lithium atoms. On the other hand, all these ceramics were tested as CO_2 captors, presenting encouraging properties through a chemisorption process. As expected, the CO_2 absorption increased as a function of total lithium contained into the ceramics. Finally, it was performed a kinetic analysis of the CO_2 absorption.

Introduction

Nowadays, energy is essential for the human being, and around 80% of it is produced from the combustion of fossil fuels. The combustion of these materials (coal, oil, and gas among others) has raised the CO_2 amounts in the atmosphere to levels never seen before.[1] As a result of that, the greenhouse effect has produced an overwarming of the earth, bringing different consequences. A possible key means for reducing the greenhouse effect is to capture, separate, and concentrate CO_2 underground.[2]

In that way, different materials have been tested as CO_2 captors: zeolites, hydrotalcites, minerals, polymers oxides and ceramics, among others,[3−9] where a specific kind of ceramics seems to present good properties: the alkaline ceramics.[10−21] The materials, of this family, that have been mainly studied as CO_2 captors are; lithium zirconates (Li_2ZrO_3 and $Li_6Zr_2O_7$),[10−13] sodium zirconate (Na_2ZrO_3)[14−16] and lithium orthosilicate (Li_4SiO_4),[17−21] among others. Additionally, it was published recently that lithium cuprate (Li_2CuO_2) is able to absorb CO_2 as well;[22] presenting as an advantage, the fact that Li_2CuO_2 captures CO_2 in a wider range of temperatures, in comparison to the other lithium ceramics mentioned previously. Finally, it should be mentioned that lithium ceramics are usually synthesized using some lithium excess, due to its tendency to sublimate at high temperatures.[23,24]

Hence, the aim of this paper was to further analyze the Li_2CuO_2 synthesis, characterization and CO_2 absorption process, giving special attention to two different aspects: (1) the effect of lithium excess on the crystalline structure, which produced $Li_{2+x}CuO_{2+x/2}$ ceramics; (2) to analyze the CO_2 capture on these lithium cuprates, $Li_{2+x}CuO_{2+x/2}$.

Experimental Section

Lithium cuprate (Li_2CuO_2) was synthesized by solid-state method. Initially, lithium oxide (Li_2O, Aldrich) and copper oxide (CuO, Acros Organics) were mixed mechanically, in order to get a good homogeneity of the reagents. Then, the powders were calcined at 800 °C for 6 h. It has been reported that lithium tends to sublimate during thermal treatments.[23,24] Hence, Li_2CuO_2 synthesis was performed using different lithium concentrations, in excess: 10, 15, 30, and 50 wt %. In fact, these nominal excess values were used to label the samples; for example, 10-Li_2CuO_2 corresponds to the sample with a lithium excess of 10 wt %.

The samples were characterized by different techniques such as powder X-ray diffraction (XRD), scanning electron microscopy (SEM), transmission electron microscopy (TEM), elemental analysis, solid state nuclear magnetic resonance (NMR) and thermogravimetric analysis (TGA). The XRD patterns were obtained with a SIEMENS D5000 diffractometer coupled to a Cu anode X-ray tube. The $K_{\alpha 1}$ wavelength was selected with a diffracted beam monochromator, and the compounds were identified conventionally using the Joint Compounds Powder Diffraction Standards (JCPDS) database. The variations on the Li_2CuO_2 cell parameters were determined by introducing an internal standard, graphite, and the selected peaks were (002), (101) and (013). SEM (Stereoscan 440, Leica-Cambridge) was used to determine the size and morphology of the particles. The samples were covered with gold to avoid a lack of electrical conductivity. A JEOL JEM-1200EX transmission electron microscope was used to obtain bright field images. The powder samples were prepared using gravimetric standard methods. The elemental composition, of the $Li_{2+x}CuO_{2+x/2}$ samples, was

* Corresponding author. Telephone: +52 (55) 5622 4627. Fax: +52 (55) 5616 1371. E-mail: pfeiffer@iim.unam.mx.
[†] Instituto de Investigaciones en Materiales, Universidad Nacional Autónoma de México.
[‡] Departamento de Química, Universidad Autónoma Metropolitana.

10.1021/jp808521f CCC: $40.75
Published on Web 12/08/2008

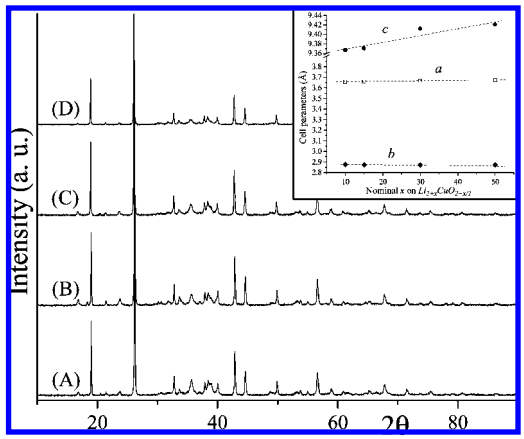

Figure 1. XRD patterns of Li_2CuO_2 synthesized with different quantities of lithium excess: (A) 10-Li_2CuO_2; (B) 15-Li_2CuO_2; (C) 30-Li_2CuO_2; (D) 50- Li_2CuO_2. The inset box shows the cell parameters of the Li_2CuO_2 samples as a function of the lithium excess.

determined by elemental analysis, which was performed in a Shimadzu equipment model AA-6200. ^{7}Li MAS NMR spectra were recorded on a Bruker Avance 300 spectrometer at 116.6 MHz, with a standard 4-mm Bruker MAS probe. The spectra acquisition consisted of a single 2 μs pulse length; with a repetition delay of 2 s. Spinning frequencies were in the range of 8.25−11.33 kHz. A total of 2000 scans were accumulated for each spectrum. Chemical shift, reported in parts per million, are relative to a 1 N aqueous solution of LiCl. Finally, thermal analyses were performed in a Hi-Res TGA 2950 thermogravimetric analyzer equipment from TA Instruments. Initially, a set of samples was heat-treated, with a heating rate of 5 °C/min, from room temperature to 1000 °C into a CO_2 flux (Praxair, grade 3.0). Additionally, another set of samples was analyzed isothermically at different temperatures; 350, 400, 450, 500, 650, 675, 700 and 725 °C. All these analyses were carried out into the same CO_2 atmosphere.

Results and Discussion

Structural Characterization. It has been reported that lithium ceramics usually loss lithium during their synthesis due to lithium sublimation as Li_2O.[23,24] Hence, in order to compensate this lithium sublimation, lithium ceramics are usually prepared with 5−10 wt % of lithium excess. In this case, different samples were prepared using 10, 15, 30 and 50 wt % of excess. XRD results are presented in Figure 1. In these results, something very interesting comes out; the excess of lithium did not seem to modify the XRD patterns of the Li_2CuO_2 phase. Li_2CuO_2 has a laminar structure formed by [CuO_4] squares, where lithium atoms are located into the interlayer spaces.[25,26] Therefore, lithium atoms, in excess, may be located at those regions producing a nonstoichiometric lithium cuprate; $Li_{2+x}CuO_{2+x/2}$. However, another option could be the formation of different lithium compounds, amorphous or nanocrystalline, which are beyond the detection limit of the XRD equipment.

The cell parameters of the different samples were measured. The inset of Figure 1 shows that, while the parameters *a* and *b* practically did not change, *c* increased significantly, as a function of the lithium excess. In fact, the parameter *c* increased from 9.3673 to 9.4211 Å. This result supports the hypothesis that at least part of the lithium excess is located into the interlayer spaces, producing the expansion of the parameter *c*.

However, in order to corroborate and further understand the location of the lithium excess, some other analyses were performed: elemental analysis and nuclear magnetic resonance of solids. The results, of the elemental analysis, are presented in Table 1. The elemental composition confirmed that although there was some lithium sublimation, most of it stayed as part of the ceramic. As it is shown on that table, the chemical formulas were normalized assuming one copper per formula, which implied the presence of some extra oxygen as well, to compensate the electroneutrality of the material. However, this technique only quantifies the metallic atoms (Li and Cu), but it does not indicate the atomic position of the lithium excess.

TABLE 1: Nominal and Real Chemical Compositions of Li_2CuO_2 Samples Containing Lithium in Excess

labeled name (Li excess wt %)	real chemical composition obtained by elemental analysis ($Li_{2+x}CuO_{2+x/2}$)[a]
10-Li_2CuO_2	$Li_{2.03}CuO_{2.015}$
15-Li_2CuO_2	$Li_{2.14}CuO_{2.07}$
30-Li_2CuO_2	$Li_{2.49}CuO_{2.25}$
50-Li_2CuO_2	$Li_{2.8}CuO_{2.4}$

[a] Chemical compositions were normalized to one copper per formula.

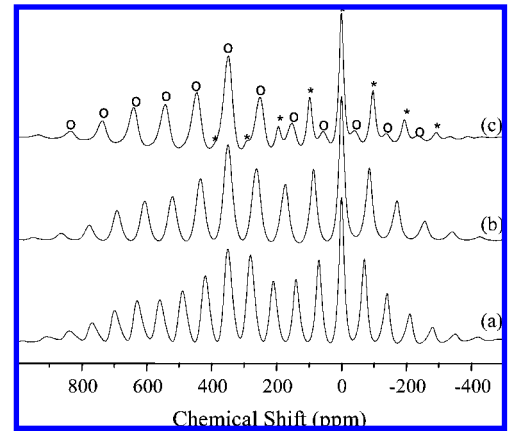

Figure 2. ^{7}Li MAS NMR spectra of the sample 10-Li_2CuO_2. Spectra were acquired at different spinning rate, (a) 8.5 kHz, (b) 10 kHz and (c) 11.5 kHz. The spinning side bands, of the signals at 0.1 and 349.9 ppm, were labeled as ∗ and ○, respectively.

Different ^{7}Li MAS NMR spectra, of the sample 10-Li_2CuO_2, are presented in Figure 2. The spectra were recorded at various spinning rate, where two isotropic signals were identified: The first one close to 0.1 ppm and the second one at 349.9 ppm. The asymmetric manifolds of spinning side bands of signal at 349.9 ppm showed the presence of large chemical shift anisotropy.

Additionally, when the lithium content increased in the Li_2CuO_2 samples, the relative intensities of the NMR signals changed as well. Specifically, as higher is the lithium excess; higher is the intensity of signal at 349.9 ppm (Figure 3). Hence, this signal should be associated to lithium atoms in excess. Thus, the signal close to 0 ppm is due to lithium ions in the Li_2CuO_2 in agreement with Nakamura.[27] Furthermore, as suggested by XRD, these NMR results strongly suggest that the second kind of lithium atoms must be hosted in the interlayer space of the [CuO_4] layers. However, the very different values of chemical shifts for the lithium species indicate that the second kind of lithium is in a different phase, where the lithium is located into a paramagnetic environment, because of the lower field position and the broader width of the peaks. Probably, the lithium is very close to oxygen atoms. In lithium oxide the distance between Li^+ and O^{2-} is expected to be close to 2 Å. Then, the

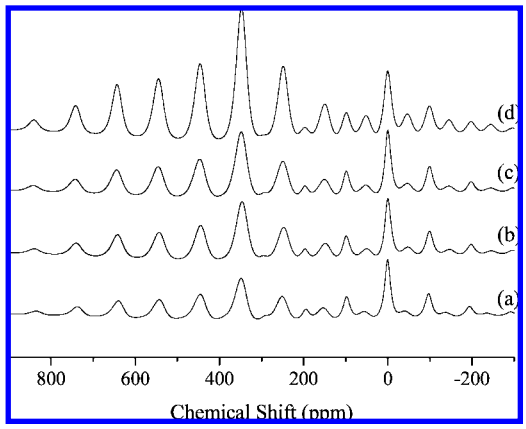

Figure 3. ^{7}Li MAS NMR of the samples (a) 10-Li_2CuO_2, (b) 15-Li_2CuO_2, (c) 30-Li_2CuO_2, and (d) 50-Li_2CuO_2.

lithium enriched phase could be a lithium oxide which is produced during the synthesis, but at same time is stabilized in the interlayer space of the [CuO_4]. This secondary phase of lithium should be homogeneously dispersed between the layers and close to Cu^{2+} cations, which are paramagnetic species.

Morphological Characterization. Figure 4 presents the morphological evolution of the samples as a function of the lithium excess. 10-Li_2CuO_2 presented a polyhedral morphology, with a particle size average equal to 3−4 μm (Figure 4A). These particles seemed to be packed, forming agglomerates and their surface did not present any kind of texture. The morphology observed, for the 15-Li_2CuO_2 and 30-Li_2CuO_2 samples (Figure 4, parts B and C), was similar to the previous one, but in these cases, the agglomerates looked denser. In other words, the particles apparently were interconnected among them by a sintering process. This phenomenon was dramatically evidenced when the lithium content was increased up to 50 wt % of excess, 50-Li_2CuO_2 (Figure 4D). In fact, this sample presented larger particles (≈20 μm) and its surface was corrugated. Summarizing, although all the samples were prepared under identical conditions, the particle size increased as a function of the lithium content. Apparently, lithium is inducing some kind of sintering. Lithium has a high mobility, which was enhanced at the synthesis temperature. Hence, as the lithium content increased it must have favored the interconnection of the particles, producing a higher sintering of the particles.

A final morphological analysis was performed by TEM. Figure 5 shows the bright field images of the 10-Li_2CuO_2 and 50-Li_2CuO_2 samples. The 10-Li_2CuO_2 sample showed the presence of relatively tiny and dense particles of around 50 nm, agglomerated among them. On the contrary, 50-Li_2CuO_2 sample showed a different aspect. The individual tiny particles, observed previously, seemed to disappear, becoming into a larger particles, which is in total agreement with the SEM observations. Additionally, this sample presented a totally different morphology. In this sample, it was depicted the formation of some kind of filament-like structures of around 10 nm thick. These structures seem to be part of the main particles, although some of them are over the surface. It may be explained in terms of the Li_2CuO_2 layered structure and the lithium addition. Apparently, lithium addition induces the growth of the Li_2CuO_2 particles with this specific kind of morphology. It may be due to the high mobility of lithium into the interlayers, which may produce the interconnection, sintering, of several particles along the interlayer axis, producing this kind of filament-like structures.

CO_2 Chemisorption Analysis. A previous paper showed that Li_2CuO_2 is able to absorb CO_2,[22] according to the following reaction:

$$Li_2CuO_2 + CO_2 \rightarrow Li_2CO_3 + CuO \quad (1)$$

Therefore, as these samples contain higher quantities of lithium, in comparison to the stoichiometric sample, they must be more reactive to the absorption of CO_2.

Indeed, Figure 6 shows that the three samples, analyzed by dynamic TGA, were able to absorb CO_2. First, 15-Li_2CuO_2 sample presented a standard CO_2 absorption according to previous report.[22] Initially, a dehydration process was observed ($T \leq 100$ °C), which was attributed merely to the evaporation of some adsorbed water molecules. At higher temperatures, two different increments of weight were detected; the first one between 240 and 400 °C, and the second one between 630 and 690 °C. Palacios-Romero and Pfeiffer[22] reported that those processes correspond to the superficial and bulk absorption processes, respectively, where the bulk absorption is activated at higher temperatures through a lithium diffusion process. Finally, at high temperatures ($T \geq 800$ °C), other two processes occur; CO_2 desorption and Li_2CuO_2 decomposition. At around 800 °C Li_2CuO_2 presented a CO_2 desorption process. But at higher temperatures, Li_2CuO_2 presented a small weight increase, which has been associated with a second absorption of CO_2 produced during lithium sublimation as Li_2O.[10] Lithium sublimation may be supported by the final weight lost, which was higher than its original weight (20 wt %), and because of the presence of lithium excess. However, another option could be the formation of metallic copper through the oxygen lost, which may be possible due to the inert CO_2 atmosphere. Actually, thermodynamic calculations suggest that CuO reduction would be more feasible than lithium oxide sublimation (reactions 2 and 3), as the equilibrium constant (K), for Li_2O vaporization, is 8 orders of magnitude smaller than that of copper reduction, at 840 °C.

$$CuO(s) \rightarrow Cu(s) + \frac{1}{2}O_2(g) \quad K = 2.16 \times 10^{-3}, \text{ at } 840\ ^\circ\text{C} \quad (2)$$

$$Li_2O(s) \rightarrow Li_2O(g) \quad K = 4.04 \times 10^{-11}, \text{ at } 840\ ^\circ\text{C} \quad (3)$$

In any case, lithium sublimation and/or copper reduction, it implies the Li_2CuO_2 decomposition at temperatures equal or higher than 840 °C under an inert CO_2 atmosphere.

In general, the CO_2 chemisorption on Li_2CuO_2 differs from that observed for other lithium ceramics, because on those ceramics (for example Li_2ZrO_3 and Li_4SiO_4) the surface and bulk absorptions are not distinguishable among them.[10,14,28−30] In other words, both processes are activated in the same interval of temperatures. Nevertheless, for Li_2CuO_2, these two processes occur at different temperatures as showed above. Consequently, it could be suggested that Li_2CuO_2 samples have a higher reactivity versus CO_2 and/or lithium diffusion is higher as well.

The results described previously were totally confirmed by 30-Li_2CuO_2 and 50-Li_2CuO_2 samples that presented similar CO_2 absorption trends. Nevertheless, these samples absorbed 2.8 and 3.4 times more CO_2 than that absorbed by 15-Li_2CuO_2, as it could be expected. The higher CO_2 absorption observed in these samples must be associated to the lithium excess of each sample; as more lithium excess, more CO_2 absorbed. Something else has to be pointed out: the increase of weight observed for the three different samples was produced between 630−690 °C, it means in the bulk that absorption was produced by the lithium diffusion. In other words, the lithium present at the surface of the particles was roughly the same for the three samples. These

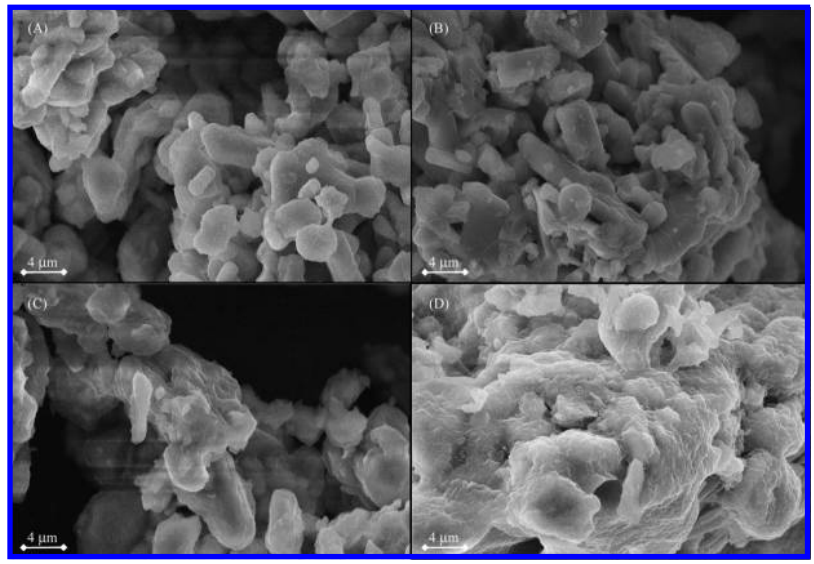

Figure 4. Scanning electron micrographs of Li_2CuO_2 synthesized with different quantities of lithium excess. (A) 10-Li_2CuO_2, (B) 15-Li_2CuO_2, (C) 30-Li_2CuO_2, and (D) 50-Li_2CuO_2.

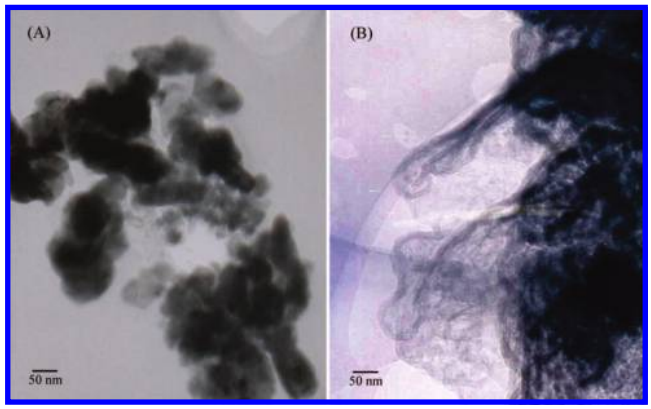

Figure 5. TEM bright field images of the 10-Li_2CuO_2 (A) and 50-Li_2CuO_2 (B) samples.

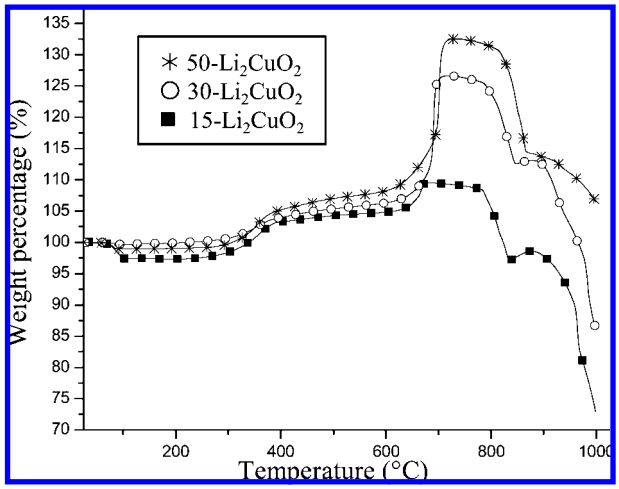

Figure 6. TGA dynamic analyses of the different lithium cuprates, containing different lithium excesses.

results strongly suggest lithium excess is mainly located into the bulk of the ceramic. This agrees with the structural characterization presented above in this manuscript. In addition, it has to be mentioned that, apparently, most of the lithium atoms are able to react with CO_2, independently of its location into the crystalline structure, which means that although the lithium atoms are stabilized into the Li_2CuO_2 material, they continue having a high mobility and reactivity under specific conditions. In that way, it has to be performed other kind of experiments, in order to evaluate the cyclability, because the crystal structure may be broken during the CO_2 absorption process inhibiting its regeneration.

On the basis of the previous results, 30-Li_2CuO_2 was analyzed isothermically at different temperatures, in order to obtain some kinetic information of one of the samples containing lithium excess. Figure 7 shows the isothermal graphs of 30-Li_2CuO_2 at different temperatures. At low temperatures (350−500 °C), the behavior observed was not the commonly expected. The isothermal at 350 °C showed an exponential behavior, which had not reached the plateau after 5 h and it had absorbed 3.95 wt %. Then, the sample treated at 400 °C presented a similar exponential behavior, but in this case, the CO_2 absorption was even slower than that observed at 350 °C. This sample only absorbed 1.82 wt %, just about the middle of the CO_2 absorbed at 350 °C. This atypical behavior, observed at low temperatures, has been already reported for the CO_2 absorption on Na_2ZrO_3.[14] This behavior was associated to a thermal shock produced on the samples during the heating process (100 °C/min, in this case), which produces a powder sintering, and therefore a significant decrement of the surface area, inhibiting the CO_2 absorption. This phenomena is only observed at low temperatures, because, once the diffusion process is activated, sintering and surface area are not preponderant factors on the CO_2 absorption any more. In these materials, it had been already proposed, according to the SEM analysis, that lithium excess induces the sintering of the particles. Therefore, this behavior totally agrees with this interpretation.

Coming back to the isothermal analysis, at 450 and 500 °C the weight gained began to increase again, absorbing 3.01 and 4.45 wt %, respectively. It means that although the sintering effect must be produced, the lithium diffusion was activated at those temperatures. On the other hand, at high temperatures (650−725 °C), the CO_2 sorption was very fast, as it could be expected. In fact, all these exponential curves reached their plateau in just a few minutes. Therefore, the lithium diffusion must be activated, and thus surface area is not a limitation for the CO_2 absorption. The best CO_2 absorption was obtained at 675 °C, while at 700 and 725 °C the CO_2 absorption decreased

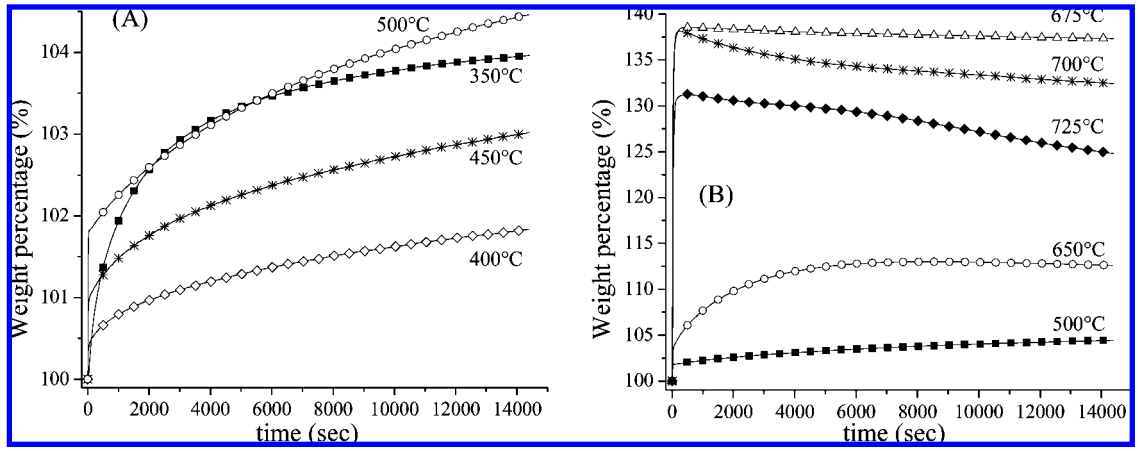

Figure 7. Isotherms of CO_2 sorption on 30-Li_2CuO_2, at different temperatures into a flux of CO_2. (A) Isotherms obtained between 350 and 500 °C. (B) Isotherms obtained between 500 and 725 °C.

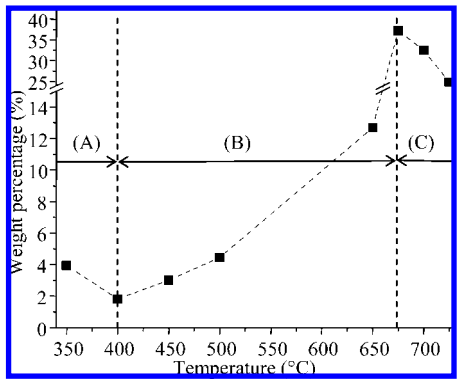

Figure 8. Tendency observed for the CO_2 saturation values at different temperatures, obtained by the extrapolation of the double exponential model fit to infinite time.

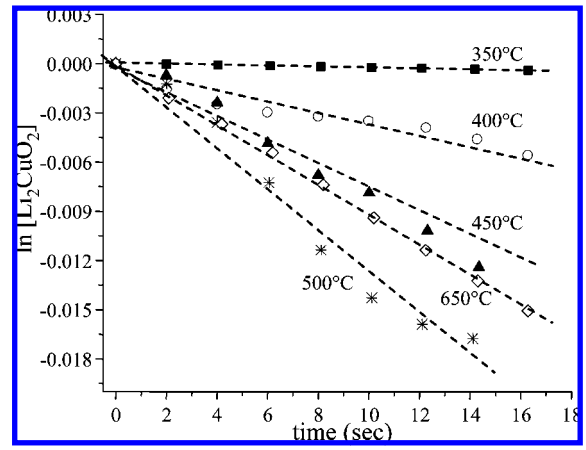

Figure 9. Plot of ln[Li_2CuO_2] vs time. The different data present a linear behavior only for short times, which correspond to the times where only the chemisorption process takes place.

appreciably. The attenuation of the CO_2 absorption, at those high temperatures, must be associated to the CO_2 absorption/desorption equilibrium. This phenomenon was observed since the sample treated at 650 °C, but it was more evident as the temperature was increased. This equilibrium is not present at lower temperatures because, there may not be desorption process. A summary of these results is presented in Figure 8, which shows the maximum CO_2 absorption at different temperatures. As can be seen, three different ranges of temperature are depicted: (1) At temperatures lower than 400 °C, the sinterization effect is preponderant over the lithium diffusion and therefore over the CO_2 chemisorption as well. As a consequence of that, the total CO_2 absorption decreases as a function of the temperature. (2) Between 400 and 650 °C diffusion process is activated and consequently the CO_2 absorption increases as a function of the temperature, because the sintering effect does not limit the processes anymore. (3) Finally, at 650 °C, or higher temperatures, although the absorption is going on, desorption process is activated limiting the CO_2 absorbed through the equilibrium process of absorption/desorption. As a consequence of that, it can be observed that the best absorption temperature was 675 °C.

In general, isothermal plots for this kind of process are usually fitted to a double exponential model, as there are two different processes taking place, chemisorption and diffusion.[14,29,31] Nevertheless, when these data were adjusted to a similar model, the results were not satisfactory at all. Data and model presented a very poor adjustment. As there is lithium excess, it could imply the presence of more and different processes. For example; two or more different lithium diffusion mechanisms may be occurring. Therefore, the kinetic data has to be analyzed by a different kind of approximation.

For the isotherms performed at low temperatures, something has to be pointed out: Although the material's sintering is decreasing the CO_2 absorption, reaction at the very first moments, seems to be increasing as a function of the temperature. Additionally, in previous papers,[14,31] it has been proposed a different kind of analysis, which implies the assumption of a first order reaction for the lithium ceramic, as CO_2 is in excess. In those papers, both analyses, double exponential and first order reaction models, fit very well among them. Therefore, in this case, it can be assumed the following model:

$$\ln[Li_2CuO_2] = -kt \qquad (4)$$

where, k is the reaction rate constant, t is the time, and [Li_2CuO_2] is the molar concentration of the ceramic. In this case, only the isotherms at low temperature were used (350−650 °C), trying to eliminate any influence produced by the desorption process, which is activated at higher temperatures. Figure 9 shows the plots of ln[Li_2CuO_2] vs time at the different temperatures. As expected, data only follow a linear behavior at short times, before the Li_2CO_3 external shell is completed and consequently the diffusion process is activated. In fact, the sample treated at 650 °C, does not follow the same trend than that showed by the other samples. It may be explained by an interference produced by the desorption process, that was evidenced on this sample.

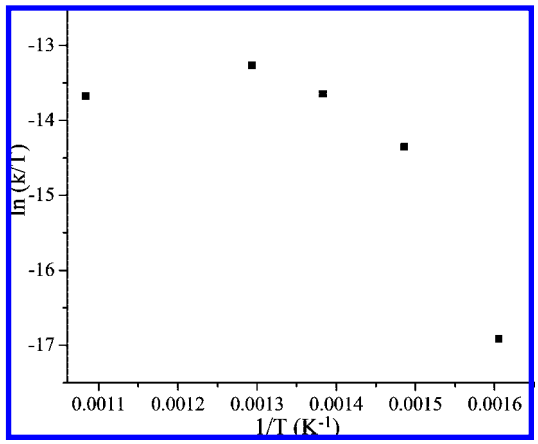

Figure 10. Eyring-type plot of ln(k/T) versus 1/T, for the data obtained assuming a first order reaction for the [Li_2CuO_2].

Usually, it has been shown that k values, obtained from Figure 9, are dependent on temperature, obtaining a straight line. However, the plot of ln(k/T) *vs* 1/T of this system presented a different behavior, Figure 10. In this case, a nonlinear trend was obtained, even if the 650 °C data is not considered, which implies that other thermodynamic or diffusion factors are influencing the reaction.

Conclusions

Lithium cuprate was synthesized by the solid state reaction, where different quantities of lithium excess were added (10, 15, 30, and 50 wt %), obtaining, in all the cases, the same crystalline structure, Li_2CuO_2. XRD results did not show the formation of any other crystalline phase different that Li_2CuO_2, but it was observed the expansion of the c cell parameter. These results suggested that lithium excess is located into the Li_2CuO_2 internal layers. ^{7}Li NMR spectra confirmed the presence of the lithium excess into the Li_2CuO_2 structure. Lithium excess is incorporated as a secondary phase, different than Li_2CuO_2. By NMR, it was clearly evidenced two different sites where lithium is located. However, from this result is difficult to propose indisputably the secondary phase. It seems that Li_2O is trapped into the structure of $Li_{2+x}CuO_{2+x/2}$, creating two different lithium environments, as detected by NMR. These results suggest that Li_2CuO_2 can be used as a cation acceptor (lithium, in this case, was demonstrated), stabilizing chemically it, but the cation is not immobilized as demonstrated by the CO_2 absorption process. In other words the cation keeps a high mobility.

Lithium excess produced changes in the morphology of the particles. The particle size increased as a function of the lithium excess and the texture of these particles became more corrugated as well (SEM). These observations were explained in terms of lithium diffusion, which is highly mobile at the synthesis temperatures, producing a high sintering process. At a nanometric scale it was possible to observe the formation of filament-like structures (TEM).

On the CO_2 absorption analyses, the samples with more lithium absorbed more CO_2, as it could be expected. The CO_2 absorption varied as a function of the lithium excess and temperature. In some cases, the efficiencies obtained were considerably high. Furthermore, all the lithium atoms were able to react with CO_2, independently of its location or chemical structure. Although lithium excess produced sintering of the ceramic particles, CO_2 absorption was not inhibited at all.

Isothermal experiments showed that the kinetic mechanism of the CO_2 absorption on Li_2CuO_2 is different to the mechanism found for other lithium ceramics. Hence, these results could not be described mathematically by the Eyring's model.

Finally, it should be mentioned that ceramics reported here ($Li_{2+x}CuO_{2+x/2}$) may have more applications than that of CO_2 absorption; for example, into the electrical field, where Li_2CuO_2 is commonly used as cathode for lithium-ion batteries or as superconductor material.

Acknowledgment. This work was financially supported by the projects 23418-SEMARNAT-CONACYT and PAPIIT-UNAM. L. M. Palacios-Romero thanks CONACYT for financial support. Authors thank to Dr. Robert Quinn, from Process and Separations Center Air Products and Chemicals Inc., for its contribution into the discussion of the Li_2CuO_2 decomposition thermodynamic data. Additionally, authors thank to L. Baños, Gerardo Cedillo, Carlos Flores, and Esteban Fregoso for technical help.

References and Notes

(1) Schrag, D. P. *Elements* **2007**, *3*, 171–178.
(2) Friedmann, S. J. *Elements* **2007**, *3*, 179–184.
(3) Pawlesa, J.; Zukal, A.; Cejka, J. *Adsorp. J. Int. Adsorp. Soc.* **2007**, *13*, 257–265.
(4) Maceiras, R.; Alves, S. S.; Cancela, M. A.; Alvarez, E. *Chem. Eng. J.* **2008**, *137*, 422–427.
(5) Romeo, L. M.; Bolea, I.; Escosa, J. M. *Appl. Therm. Eng.* **2008**, *28*, 1039–1046.
(6) Siauciunas, R.; Rupsyté, E.; Kitrys, S.; Galeckas, V. *Colloids Surf. A: Physicochem. Eng. Asp.* **2004**, *244*, 197–204.
(7) Chen, J.; Loo, L. S.; Wang, K. *J. Chem. Eng. Data* **2008**, *53*, 2–4.
(8) Nomura, K.; Tokumistu, K.; Hayakawa, T.; Homonnay, Z. *J. Radioanal. Nucl. Chem.* **2000**, *246*, 69–77.
(9) Park, S. W.; Cho, H. B.; Sohn, I. J.; Kumazawa, H. *Sep. Sci. Technol.* **2002**, *37*, 639–661.
(10) Pfeiffer, H.; Bosch, P. *Chem. Mater.* **2005**, *17*, 1704–1710.
(11) Nair, B. N.; Yamaguchi, T.; Kawamura, H.; Nakao, S. I. *J. Am. Ceram. Soc.* **2004**, *87*, 68–74.
(12) Ochoa-Fernández, E.; Rønning, M.; Yu, X.; Grande, T.; Chen, D. *Ind. Eng. Chem. Res.* **2008**, *47*, 434–442.
(13) Yi, K. B.; Eriksen, D. Ø. *Sep. Sci. Technol.* **2006**, *41*, 283–296.
(14) Alcérreca-Corte, I.; Fregoso-Israel, E.; Pfeiffer, H. *J. Phys. Chem. C* **2008**, *112*, 6520–6525.
(15) Zhao, T.; Ochoa-Fernández, E.; Rønning, M.; Chen, D. *Chem. Mater.* **2007**, *19*, 3294–3301.
(16) Pfeiffer, H.; Vazquez, C.; Lara, V. H.; Bosch, P. *Chem. Mater.* **2007**, *19*, 922–926.
(17) Khomane, R. B.; Sharma, B. K.; Saha, S.; Kulkarni, B. D. *Chem. Eng. Sci.* **2006**, *61*, 3415–3418.
(18) Gauer, C.; Heschel, W. *J. Mater. Sci.* **2006**, *41*, 2405–2409.
(19) Yamaguchi, T.; Niitsuma, T.; Nair, B. N.; Nakagawa, K. *J. Membr. Sci.* **2007**, *294*, 16–21.
(20) Kato, M.; Nakagawa, K.; Essaki, K.; Maezawa, Y.; Takeda, S.; Kogo, R.; Hagiwara, Y. *Int. J. Appl. Ceram. Tech.* **2005**, *2*, 467–475.
(21) Kato, M.; Maezawa, Y.; Takeda, S.; Hagiwara, Y.; Kogo, R.; Semba, K.; Hamamura, M. *Key Eng. Mater.* **2006**, *317−318*, 81–84.
(22) Palacios-Romero, L. M.; Pfeiffer, H. *Chem. Lett.* **2008**, *37*, 862–863.
(23) Pfeiffer, H.; Knowles, K. M. *J. Eur. Ceram. Soc.* **2004**, *24*, 2433–2443.
(24) Antolini, E.; Ferretti, M. *J. Solid State Chem.* **1995**, *117*, 1–7.
(25) Owens, F. J. *Physica C* **1999**, *313*, 65–69.
(26) Kawamata, S.; Okuda, K.; Kindo, K. *J. Magn. Magn. Mater.* **2004**, *272*, 939–940.
(27) Nakamura, K.; Moriga, T.; Sumi, A.; Kashu, Y.; Michihiro, Y.; Nakabayashi, I.; Kanashiro, T. *Solid State Sci.* **2005**, *176*, 837–840.
(28) Choi, K. H.; Korai, Y.; Mochida, I. *Chem. Lett.* **2003**, *32*, 924–925.
(29) Venegas, M. J.; Fregoso-Israel, E.; Escamilla, R.; Pfeiffer, H. *Ind. Eng. Chem. Res.* **2007**, *46*, 2407–2412.
(30) Kato, M.; Nakagawa, K. *J. Ceram. Soc. Jpn.* **2001**, *109*, 911–914.
(31) Mosqueda, H. A.; Vazquez, C.; Bosch, P.; Pfeiffer, H. *Chem. Mater.* **2006**, *18*, 2307–2310.

JP808521F